

ON THE COMPUTATION OF SEISMIC FRAGILITY CURVES

F. Colangelo

Associate Professor, DISAT Dept., University of L'Aquila, Monteluco di Roio, Italy
Email: col@ing.univaq.it

ABSTRACT:

Seismic damage assessment is dealt with in terms of fragility curves. Several approaches for their evaluation, including first-order reliability and a fuzzy random method, are reviewed. These methods are applied to a deterministic infilled reinforced-concrete frame, and the resulting fragility curves compared. Aim is to appraise empirically any difference. Nonstructural damage of the infill is considered. It is assumed to be correlated with the peak interstory drift ratio and dependent on the peak ground acceleration. It is concluded that randomness of the capacity is essential. If a damage state is associated with a deterministic drift range, then fragility steeply increases with the peak ground acceleration, and it is quite overestimated. Comparatively, any other difference among the considered methods results to be minor.

KEYWORDS: Fragility curve, lognormal distribution, infilled frame, nonstructural damage, interstory drift

1. INTRODUCTION

Quantification of the seismic damage is essential, particularly for the buildings (Hwang and Jaw, 1990; Mosalam et al., 1997; Singhal and Kiremidjian, 1996). Before the occurrence of earthquakes, predicting damage scenarios may address the planning of strengthening and upgrading. After a destructive earthquake, measurement of damage on individual buildings may result in declaring their immediate functionality or the need for abandoning them. Post-earthquake damage assessment may also suggest the choice among repairing, retrofitting, or demolishing and rebuilding.

The damage measure depends on the ground motion, both the response and the capacity of the building itself, and the damage index. Many uncertainties affect them, thus a probabilistic assessment seems to be proper. Basically, such an approach involves two quantities: the hazard at the site and the vulnerability of the building. This work deals with the second one only. Vulnerability is characterized by analytical fragility curves conditional on the earthquake intensity.

A number of methods exist for deriving the fragility curves. Aim of this work is briefly reviewing several approaches, and comparing empirically the fragility curves obtained by such methods, once applied to a same benchmark structure. This is a deterministic four-story masonry-infilled reinforced-concrete (RC) frame, modeled member by member and analyzed under artificial accelerograms. The infill damage is considered. The peak interstory drift ratio is adopted as the damage index. The intensity of the ground motion is characterized in terms of the peak ground acceleration (PGA).

2. METHODS FOR FRAGILITY EVALUATION

Mathematically, fragility is the probability of attaining or exceeding a certain damage state, conditional on the ground motion intensity. In the case of analytical evaluation, discrete values of this probability are obtained by numerical simulation, and related statistical inference, of the demand D at discrete ground motion intensities $G = g_j$ given the capacity C_i against every damage state i . Symbolically, one can write such discrete values of fragility as follows:

$$P_{ij} = P\{D \geq C_i | G = g_j\} \quad (2.1)$$

Capacity may be assumed to be either deterministic or random. In the former case, C_i in Eqn. 2.1 is the threshold value

associated with the onset of the damage state i . This is quantified by a proper damage index.

The fragility curve expresses the exceeding probability as a continuous function of the ground motion intensity, that is $P_i = P_i(G)$. Usually, this is the smooth function that fits best, in some sense, the discrete values of probability versus those of the ground motion intensity. Various methods used to identify a fragility curve are mentioned in the next sections. All in all, Eqn. 2.1 is worthy of a greater attention with respect to the problem of fitting the probability values.

2.1. Relative Frequency (RF) Method

Capacity is assumed to be deterministic. The exceeding probability is approximated by the relative frequency, that is:

$$P_{ij} = n_{ij} / N \quad (2.2)$$

n_{ij} is the number of demands found to exceed the capacity C_i among the performed N realizations at the ground motion intensity g_j . The fragility curves pertaining to each damage state i derive from least-squares fitting of such cumulative relative frequencies. For instance, Mosalam et al. (1997) assumed an exponential fitting model. This is a crude, quite simple method characterized by being independent of any particular probability distribution of the realizations.

2.2. Lognormal Distribution (LD) Method

Capacity is assumed to be deterministic. The realizations are assumed to follow some probability distribution function, to be identified specifically to both the damage state and the ground motion intensity. Eqn. 2.1 writes:

$$P_{ij} = 1 - F_{ij}(C_i) \quad (2.3)$$

F_{ij} is the cumulative probability distribution function. It is common to use the two-parameter lognormal distribution. Singhal and Kiremidjian (1996) verified such assumption at a 5% confidence level by the Kolmogorov-Smirnov test, and assumed a lognormal distribution function to express the fragility curves as well, identified by ordinary fitting.

2.3. Maximum Likelihood (BD) Method

Capacity is assumed to be deterministic. Following Shinozuka et al. (2000), each realization is interpreted as the result of a multi-outcome Bernoulli-type experiment, in the sense that it resolves a dichotomy for a number of events. In fact, each damage state i results to be at least attained in the realization, or contrarily it is not. Similarly to the LD method, a lognormal distribution function is assumed to express the fragility curves. They are formulated as follows:

$$P_i = \Phi \left(\frac{1}{a_i} \ln \frac{G}{b_i} \right) \quad (2.4)$$

Φ is the standard normal cumulative distribution function. a_i and b_i are the parameters specific to each damage state i . Distinctive of this method is that the parameters are identified on a consistent, rational basis, so that a fragility curve is more than a mere least-squares fitting function. In fact, the parameters maximize the following likelihood function:

$$L_i = \prod_{jk} P_i^{\delta_{ijk}} (1 - P_i)^{1 - \delta_{ijk}} \quad (2.5)$$

δ_{ijk} is either 1 or 0 depending on whether or not the damage state i is at least attained under the ground motion intensity

g_j in the realization k . Computationally, it is convenient to maximize the logarithm of L_i . Shinozuka et al. (2000) used a straightforward optimization algorithm. In this work, the Powell algorithm is used to solve the nonlinear equations:

$$\begin{cases} \partial \ln L_i / \partial a_i = 0 \\ \partial \ln L_i / \partial b_i = 0 \end{cases} \quad (2.6)$$

2.4. First-order Second-moment (FS) Method

Both demand and capacity are treated as random variables. According to the *full distributional approach*, it is:

$$P_{ij} = \iint_{C_i \leq D_j} f_{C_i, D_j}(c, d) dc dd \quad (2.7)$$

f_{CD} is the joint probability density function of capacity and demand. Assumed that they are independent and lognormal, Eqn. 2.7 reduces to the first-order reliability basic formulation in terms of the second moments of the distributions:

$$P_{ij} = \Phi \left(- \frac{\mu_{\ln C_i} - \mu_{\ln D_j}}{\sqrt{\sigma_{\ln C_i}^2 + \sigma_{\ln D_j}^2}} \right) \quad (2.8)$$

μ_{\ln} and σ_{\ln} are the log-parameters of the distributions. Among others, Hwang and Jaw (1990) adopted this approach.

2.5. Fuzzy Random (FR) Method

Often the damage quantification seems to be naturally fuzzy, especially if the damage scale is descriptive. For instance, it may be not clear whether to classify a certain level of concrete crushing and cracking as moderate damage or heavy damage, a certain member as repairable or to be replaced. Formally, a certain condition may belong to more than one damage state, with some *degree of membership* to each. Exceeding a damage state i becomes a fuzzy random event. From basic theory, its probability is the expectation of the membership function μ_E relevant to this event, i.e.:

$$P_{ij} = \iint_{\infty} \mu_{E_i}(c, d) f_{C_i, D_j}(c, d) dc dd \quad (2.9)$$

Gu and Lu (2005) assumed the membership function μ_E to be the normalized integral of a piecewise second-degree Bernstein polynomial. In this work, the following piecewise second-degree Bernstein polynomial is directly assumed:

$$\mu_{E_i}(c, d) = \begin{cases} 0 & d \leq (1 - \gamma_i)c \\ \frac{1}{2} \left[\frac{d - (1 - \gamma_i)c}{\gamma_i c} \right]^2 & (1 - \gamma_i)c \leq d \leq c \\ 1 - \frac{1}{2} \left[\frac{(1 + \gamma_i)c - d}{\gamma_i c} \right]^2 & c \leq d \leq (1 + \gamma_i)c \\ 1 & (1 + \gamma_i)c \leq d \end{cases} \quad (2.10)$$

γ_i is a parameter that regulates the steepness of the membership function of the damage state i , that is its fuzziness. Under the additional assumption that capacity and demand are independent and lognormal, Eqn. 2.9 reduces to a sum of nine one-dimensional convolution integrals involving the standard normal cumulative distribution function.

2.6. Evaluation of the Lognormal Distribution Parameters

Capacity and demand involved in the damage assessment are non-negative, thus they are often assumed to follow a two-parameter lognormal distribution. Three approaches may be adopted to estimate its parameters: the moment (M) method, the maximum-likelihood (ML) method, and the least-squares (LS) method (Stoica et al., 2007).

According to the M method, the population mean and the population standard deviation are respectively approximated by the sample average and by the sample standard deviation. Then basic relations about moments are used to obtain the log-mean and the log-standard deviation. The ML method considers statistics of the logarithms of the realizations, rather than the realizations themselves. Thus the log-mean and the log-standard deviation are directly estimated as the sample average and the sample standard deviation, respectively. Finally, the LS method estimates the log-parameters by least-squares optimization. First, realizations are sorted in ascending order. The cumulative probability associated with the realization at position m is assumed to equal its cumulative relative frequency $m/(N+1)$. The inverse of the standard normal cumulative distribution function at such probabilities gives the values of a standard normal variable corresponding to the realizations. Least-squares fitting of the realizations versus the standard normal variable gives the log-parameters (e.g., see Hwang and Jaw, 1990). Both exponential and equivalent linear regression models may be used for this purpose. Alternatively, the log-parameters may be evaluated by iteration, aiming to minimize the sum of the squares of the differences between the cumulative relative frequency and the theoretical cumulative probability consistent with the current log-parameter values (Stoica et al. 2007).

Stoica et al. (2007) found that the accuracy of the methods was similar in many cases. The LS method (applied in its latter formulation only) provided the best accuracy, even much greater than that of the other methods in some cases. In this work, the LS method in its former formulation only is applied, together with the M and ML methods.

3. BENCHMARK INFILLED-FRAME STRUCTURE

The aforesaid methods are applied to a four-story three-bay RC frame of a residential building. Stories are 3m high, spans are 5m long. The beam cross-section is 30×50cm everywhere. At levels 1 and 2, the outer column cross-section is 50×50cm, the inner column cross-section is 55×55cm. At levels 3 and 4, the lengths of the column cross-section are 5cm lesser. This frame is designed according to Eurocodes (European Committee for Standardization, 2004a, b) with a modal response-spectrum seismic analysis. The concrete average compressive strength is 33MPa, the steel average yield strength is 530MPa. Dead load amounts to 32kN/m on the residential floors, 24kN/m on the roof. Live load amounts to 8kN/m everywhere. The seismic design ductility class is *medium*. The corresponding *behavior factor* equals 3.9. The design PGA is 0.25g times an amplification factor equal to 1.35 due to the present ground type.

The RC frame is uniformly infilled by nonstructural masonry walls made of perforated bricks and cement mortar. These walls are 16cm thick. The masonry shear modulus is 1.1GPa, its Young modulus is 2.0GPa. The shear strength is 1.0MPa, the compressive strength is 5.0MPa. All properties are assumed to be deterministic.

3.1. Hysteretic Model

In order to carry out the non-linear time-history analyses for fragility computation, the frame members are modeled one-to-one as linearly elastic beam elements. Their stiffness is one half of the stiffness associated with the concrete gross, uncracked cross-section (European Committee for Standardization, 2004b). Each beam element is provided with two rigid-plastic point springs located at its ends. The spring cyclic behavior follows the model by Takeda as simplified by Otani and by Litton (CEB, 1996), with the model parameters β and α assumed equal to 0 and 0.4, respectively. The yield bending moments are calculated using the average strength of concrete and reinforcing steel. The strain hardening ratio referred to the member load-displacement curve is defined to be 1.0% for the beams, and 0.5% for the columns.

Infill walls are modeled as a pair of diagonal struts connecting the frame joints. The hysteretic model by Panagiotakos

and Fardis (Fardis, 1997) in its second version is assumed. This is a multi-linear phenomenological model including first cracking, pinching, strength decrease in reloading and deterioration of the envelope curve. Additional information on the model calibration and parameter values can be found elsewhere (Colangelo, 2003).

Linear viscous damping is defined as proportional to both the mass and the initial stiffness matrix of the infilled frame. In the linearly elastic response, it equals 5% for the first and the third mode of oscillation in the horizontal direction.

3.2. Capacity of the Infill Wall

The infill damage is descriptively classified into four levels of severity. These levels are named minor, moderate, major, and complete damage. Minor damage consists in the first cracking of the infill. Moderate damage corresponds to extensive, wide cracks in the infill, however before attaining its peak strength. Major damage is reached as a few bricks exhibit splitting and falling out of their outer layer. Repairing of the infill is reasonable still. In the complete damage, so many bricks have been broken as attempting to repair the infill is unreasonable, and rebuilding is necessary.

The infill capacity against the aforesaid damage states is assumed on the basis of pseudo-dynamic tests carried out with one-bay one-story infilled-frame specimens scaled 1:2 (Colangelo, 2005). In fact, the model outlined in Section 3.1 was calibrated so that its results are in reasonable agreement with the experimental ones (Colangelo, 2003). Capacity was identified by statistical processing of both the experimental and numerical results (Colangelo and Stornelli, 2006).

Many damage indices exist in the literature. In this work, the peak interstory drift ratio is adopted. Its lognormal probability density function and membership function have the parameter values listed in Table 1. They are illustrated in Figure 1. Symbols mark every observation of the drift at a damage state, as measured in the pseudo-dynamic tests. In the case of deterministic capacity, the drift range associated with each damage state is assumed to be bounded by the drift values where the probability density functions intersect each other. The drift value causing the onset of minor damage is assumed to be the same (lower) percentile as that distinguishing minor damage from moderate damage.

4. GROUND MOTION

Code-compatible artificial accelerograms are used in the nonlinear dynamic analyses. They consist of truncated cosine series with stationary frequency content. Following Vanmarcke (Lomnitz and Rosenblueth, 1976), the power spectral density function is identified by iteration, until the elastic response spectrum derived by the peak factor matches the design elastic response spectrum to a reasonable degree of accuracy. Intensity is made non-stationary by a trapezoidal modulating function. The total duration is twice that of its stationary part, which is assumed to linearly increase from 10s to 25s as the PGA increases from 0.1g to 0.4g. Outside this range, the duration is kept equal to its bounding values.

5. ESTIMATED FRAGILITY CURVES

5.1. Number of Realizations

In order to represent the design seismic action, Eurocode (European Committee for Standardization, 2004b) prescribes a minimum of three artificial accelerograms. As a matter of fact, ten or so accelerograms generated as previously said give an average acceleration elastic response spectrum in a good agreement with the design spectrum. However, a much greater number of analyses results to be necessary to obtain stable statistics of the drift ratio, its dispersion more than its average. This is shown in Figures 2 and 3. In addition, the proper sample size increases with increasing the PGA (and duration as well, Section 4). This seems related to the degree of nonlinearity in the response. In fact, Figures 2 and 3 show that as soon as the drift at some story exceeds the first cracking value, the relevant standard deviation to a great extent increases, and it needs more realizations to become stable (please note that the axis scales are different). The inherent degree of nonlinearity is perceived in Figure 4. In the following, 100 realizations are treated at each PGA.

5.2. Lognormal Distribution Parameters

Preliminarily, the lognormal distribution is found to fit the peak drift ratio a little better than the normal distribution. This is shown in Table 2, where the coefficients of determination calculated by the LS method for both distributions are listed. Higher values denote that the regression curve is a little more effective in explaining the total variation about the mean in the case of lognormal distribution. A similar result was previously found for the capacity (Colangelo and Stornelli, 2006). Referring to the lognormal distribution, the M, ML, and LS methods yield the parameter values reported in Tables 3 and 4. All in all, if one aims to practically evaluate the (relatively great) probability related to a seismic fragility curve, the three methods result to be equivalent. The M method is used to derive the fragility curves in the next section.

5.3. Fragility Curves

The fragility curves of the first story, that is where damage would be concentrated in the case of uniformly infilled frames, are plotted in Figure 5. It appears that differences between the RF and LD methods are insignificant, again as long as one is interested in evaluating the seismic fragility. In fact, the relative frequency, Eqn. 2.2, almost coincides with the exceeding probability by lognormal distribution, Eqn. 2.3. Any difference with the BD method is small as well, at the greater damage states especially for this story. The FS method suggests the damage to start under a similar PGA. However, sensitivity to the PGA is much lower, and fragility is much less thereafter. This remark also applies to the FR method, therefore this difference seems due to having considered a random capacity, rather than fuzziness. Assuming the threshold drift value that defines capacity to equal the mean value of the lognormal distributions, rather than the lower bound of the drift range said in Section 3.2, causes the LD curves to shift to the right (please look at the dashed lines). The LD curve intersects both the FS and FR curves now, however its greater steepness remains.

6. CONCLUSIONS

A number of approaches to derive seismic fragility curves have been mentioned and applied to a single infilled-frame structure. The resulting fragility curves are compared empirically. Damage of the nonstructural infill wall is considered, in correlation with the peak interstory drift ratio and depending on the PGA. From the practical point of view, certain fragility curves almost coincide, thus complexity of some formulations appears to be redundant. The outstanding result is that considering randomness of the capacity is essential. Fuzziness seems to be not as important. If a threshold drift value is associated with the damage occurrence, then the fragility steeply increases with the PGA. If the lower bound of a range of possible drift values is assumed, then the fragility is overestimated, to a quite conservative degree.

REFERENCES

- CEB Bulletin 231 (1996). RC Frames under Earthquake Loading, Telford, London.
- Colangelo, F. (2003). Experimental evaluation of member-by-member models and damage indices for infilled frames. *Journal of Earthquake Engineering* **7:1**, 25-50.
- Colangelo, F. (2005). Pseudo-dynamic seismic response of RC frames infilled with nonstructural brick masonry. *Earthquake Engineering and Structural Dynamics* **34**, 1219-1241.
- Colangelo, F. and Stornelli, P. (2006). Seismic damage of nonstructural masonry infills: statistical characterization by interstory drift and stiffness decrease. *Proc. 8th U.S. National Conf. on Earthquake Engineering*, Paper no. 821.
- European Committee for Standardization (2004a). Eurocode 2: Design of Concrete Structures, CEN, Brussels.
- European Committee for Standardization (2004b). Eurocode 8: Design of Structures for Earthquake Resistance, CEN,

Brussels.

Fardis, M.N. editor (1997). Experimental and Numerical Investigations on the Seismic Response of RC Infilled Frames and Recommendations for Code Provisions, Laboratorio Nacional de Engenharia Civil, Lisbon.

Gu, X. and Lu, Y. (2005). A fuzzy-random analysis model for seismic performance of framed structures incorporating structural and nonstructural damage. *Earthquake Engineering and Structural Dynamics* **34**, 1305-1321.

Hwang, H.H.M. and Jaw, J.-W. (1990). Probabilistic damage analysis of structures. *Journal of Structural Engineering* **116:7**, 1992-2007.

Lomnitz, C. and Rosenblueth, E. editors (1976). Seismic Risk and Engineering Decisions, Elsevier, Amsterdam.

Mosalam, K.M., Ayala, G., White, R.N. and Roth, C. (1997). Seismic fragility of LRC frames with and without masonry infill walls. *Journal of Earthquake Engineering* **1:4**, 693-720.

Shinozuka, M., Feng, M.Q., Lee, J. and Naganuma, T. (2000). Statistical analysis of fragility curves. *Journal of Engineering Mechanics* **126:12**, 1224-1231.

Singhal, A. and Kiremidjian, A.S. (1996). Method for probabilistic evaluation of seismic structural damage. *Journal of Structural Engineering* **122:12**, 1459-1467.

Stoica, M., Medina, R.A. and McCuen, R.H. (2007). Improved probabilistic quantification of drift demands for seismic evaluation. *Structural Safety* **29**, 132-145.

Table 1 Parameter values of the infill capacity in terms of the peak drift ratio

Damage state	Minor	Moderate	Major	Complete
Drift mean value [%]	0.03	0.40	0.80	1.60
Drift standard deviation [%]	0.02	0.30	0.40	0.40
Fuzziness parameter γ (Eqn. 2.10)	0.95	0.97	0.91	0.70

Table 2 Coefficient of determination [%] of the normal and lognormal distributions of the peak drift ratio

PGA Story	0.2g				0.3g				0.4g				0.5g			
	1 st	2 nd	3 rd	4 th	1 st	2 nd	3 rd	4 th	1 st	2 nd	3 rd	4 th	1 st	2 nd	3 rd	4 th
Normal	98.2	98.2	97.7	97.3	84.1	97.2	96.2	97.7	96.5	98.3	71.3	97.4	96.5	91.5	88.3	99.2
Lognormal	98.6	98.6	98.8	98.5	90.4	98.1	98.0	98.7	97.7	92.0	81.5	98.5	99.5	96.9	98.1	99.2

Table 3 Mean value of the peak drift ratio [%] according to the M, ML, and LS methods

PGA Story	0.2g				0.3g				0.4g				0.5g			
	1 st	2 nd	3 rd	4 th	1 st	2 nd	3 rd	4 th	1 st	2 nd	3 rd	4 th	1 st	2 nd	3 rd	4 th
M method	0.02	0.02	0.02	0.01	0.04	0.04	0.03	0.02	0.37	0.36	0.06	0.03	0.83	0.78	0.28	0.04
ML method	0.02	0.02	0.02	0.01	0.04	0.04	0.03	0.02	0.37	0.36	0.06	0.03	0.83	0.78	0.28	0.04
LS method	0.02	0.02	0.02	0.01	0.04	0.04	0.03	0.02	0.37	0.36	0.05	0.03	0.83	0.78	0.29	0.04

Table 4 Coefficient of variation [%] of the peak drift ratio according to the M, ML, and LS methods

PGA Story	0.2g				0.3g				0.4g				0.5g			
	1 st	2 nd	3 rd	4 th	1 st	2 nd	3 rd	4 th	1 st	2 nd	3 rd	4 th	1 st	2 nd	3 rd	4 th
M method	7.4	6.3	8.2	10.2	20.1	5.6	7.7	7.1	22.9	24.2	35.3	8.3	23.5	22.4	36.3	9.3
ML method	7.4	6.3	8.2	10.1	18.3	5.6	7.6	7.0	23.4	28.1	29.1	8.3	23.3	21.2	34.6	9.4
LS method	7.6	6.5	8.4	10.4	18.0	5.7	7.8	7.2	24.0	27.9	27.1	8.5	24.1	21.6	35.6	9.7

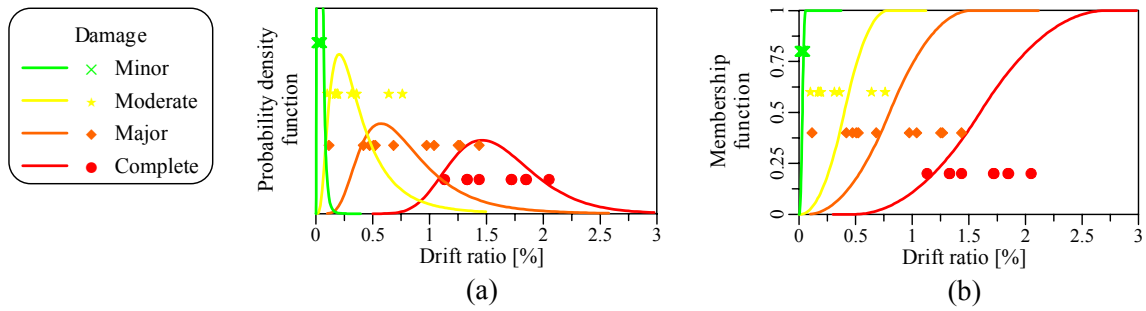


Figure 1 Probability density functions (a) and membership functions (b) of the infill capacity

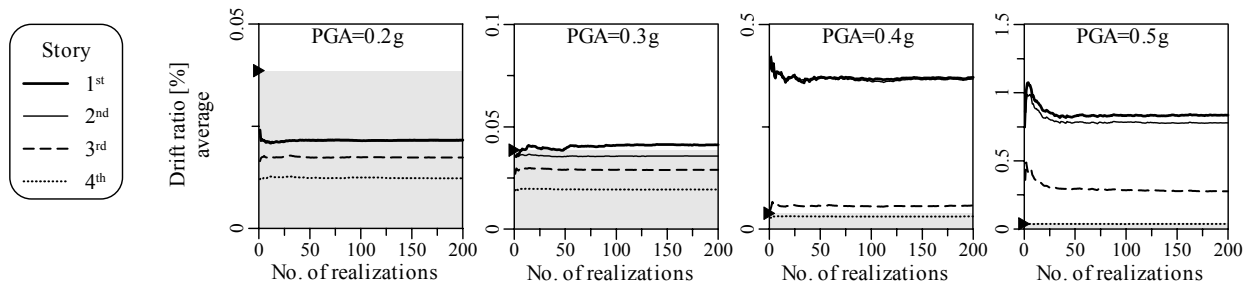


Figure 2 Sample average of the peak drift ratio; the symbol “▶” marks the infill first cracking drift

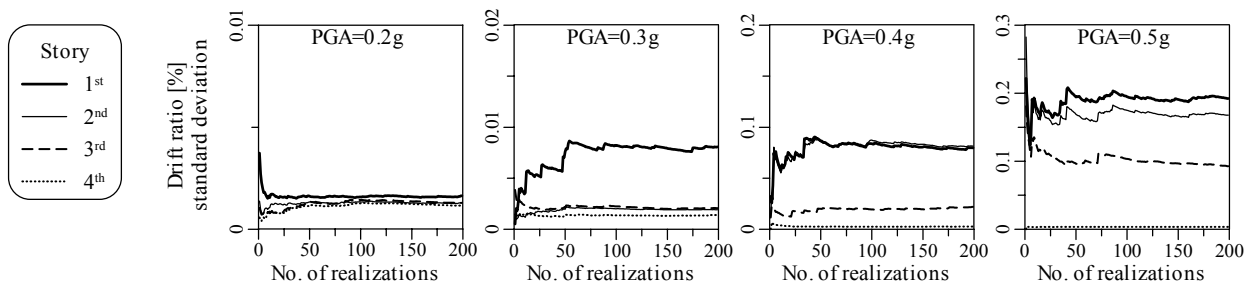


Figure 3 Sample standard deviation of the peak drift ratio

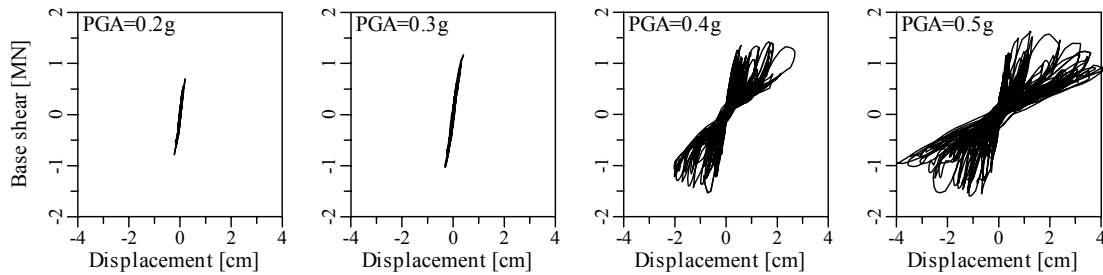


Figure 4 Base shear versus roof displacement, realizations no. 42

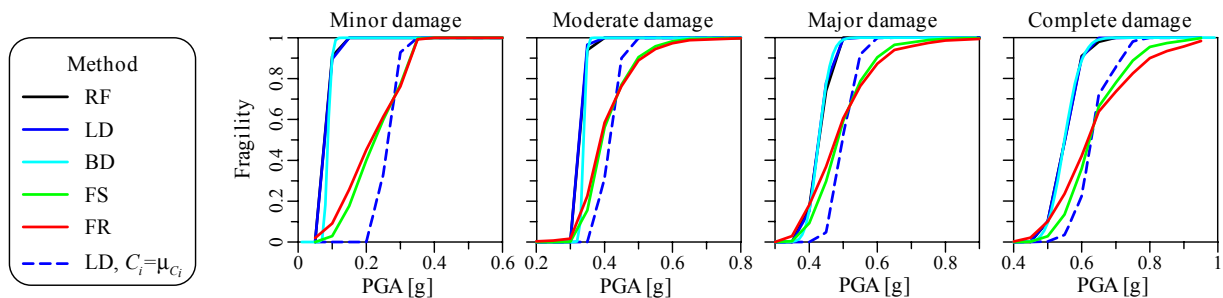


Figure 5 Fragility curves of the first story